DIGITAL TECHNOLOGIES FOR STEEL MANUFACTURING (DTSM) GRANT

Final Report.. 2025-2026

AI-Driven Radiative Sensing for Optimizing Continuous Galvanizing Processes

Principal Investigator
Dr. Fatima K. Suleiman | Postdoctoral Fellow
Department of Mechanical and Mechatronics Engineering
University of Waterloo, Canada
Email: fsuleiman@uwaterloo.ca

Supervising Professor
Prof. Kyle J. Daun
Department of Mechanical and Mechatronics Engineering
University of Waterloo, Canada
Email: kjdaun@uwaterloo.ca
Website: uwaterloo.ca/watlit

Research Team
Dr. Malo Lecorgne | Postdoctoral Fellow
Michiyo Kagaya | MASc Student, Mechanical Engineering
Ardhendu Bhattacharya | MASc Student, Mechanical Engineering
Andrew Jackson Leach | Undergraduate Student, Mechanical Engineering

Industry Mentor
Christopher Martin-Root
Stelco Hamilton Works, Canada
Email: Christopher.Martin-Root@stelco.com

Executive Summary

Continuous galvannealing lines rely on precise thermal control to arrive at a coating that provides the required downstream functionalization. Temperature must be inferred through spectral irradiance measurements via pyrometry, which requires knowledge of the emissivity of the surface. This process is challenging since the radiative properties of the surface change significantly as it evolves from a liquid metal into a rough solid coating composed of various intermetallic phases. However, the sensitivity of the radiative properties to the surface state also presents an opportunity to measure the evolving coating *in-situ*. This information, combined with concurrent advances in optoelectronics, machine learning, artificial intelligence, and high-performance computing, presents an opportunity for more robust sensing and quality-control technologies for advanced steel manufacturing.

The objective of this project is to develop a knowledge foundation to support the development of such a system, specifically focused on elucidating the relationship between emissivity and surface condition during the galvannealing of zinc coated, interstitial-free (IF) steel. Laboratory experiments were conducted to generate a phase- and composition-resolved emissivity dataset spanning the near-infrared (NIR), mid-infrared (MIR), and long-wave infrared (LWIR) spectral regions. These datasets were combined with metallurgical characterization, including SEM/EDS analysis, ICP measurements of coating iron (Fe) content, and surface-topography measurements, to identify the physical factors governing emissivity evolution during galvannealing.

The results showed that emissivity evolves systematically with galvannealing progression and exhibits a strong relationship with coating Fe content. Spectral emissivity features in selected LWIR bands demonstrated strong sensitivity to coating Fe content. Machine-learning models developed using these spectral descriptors were able to predict coating Fe content with good accuracy on both laboratory and industrial samples.

The project delivered a composition-resolved emissivity library for galvannealed IF steel, identified spectral regions most sensitive to coating evolution, and demonstrated the feasibility of using radiative properties as a non-contact, non-destructive indicator of galvannealing progression. These findings establish a foundation for future development of intelligent sensing technologies capable of supporting real-time monitoring and quality control in continuous galvanizing lines.

1. Introduction

Automakers rely on advanced high strength steels to develop lighter and more fuel-efficient vehicles without compromising crash performance and passenger safety. However, the thinner cross-sections enabled through the mechanical performance of these alloys means that they must be protected against any additional material loss through corrosion. Continuous galvanizing and galvannealing are effective means of accomplishing this goal. In galvanizing the steel sheet exits an atmosphere-controlled inter-critical annealing process beneath the surface of a zinc pot. The strip emerges from the zinc pot and flows through air knives, which are used to control the coating thickness.

In the case of galvanizing, the liquid zinc coating is allowed to solidify, while galvannealed coatings are produced by passing the strip through an additional radiative or inductive heating stage that allows iron from the substrate steel to diffuse into the zinc coating, where zinc and iron atoms react to form a sequence of intermetallic compounds. The downstream performance of the galvannealed coating, especially in terms of weldability, paint adhesion, formability, and corrosion resistance, depends on attributes that include coating roughness, thickness, and the constitutive intermetallic compounds (gamma, delta, zeta), which are often summarized by the iron percentage within the coating.

These properties depend strongly on the temperature history of the coating, which is controlled via the power input to the heating stage and the line speed. These parameters must be adjusted to maximize production rate while ensuring a galvannealed coating that maintains its downstream functionality. This is mainly done through a combination of operator experience, online pyrometry, and offline *ex-situ* measurements (e.g., optical emission spectroscopy on specimens excised from the head or tail of the coating), but this technique is far from optimal, often resulting in lower throughput or product having deficient properties.

A further complication concerns the accuracy of temperature measurement, which relies on precise knowledge of the radiative properties of the galvanneal coating. However, these properties change dramatically as the coating evolves from a smooth liquid metal to a solid, rough material composed of multiple intermetallic phases. To address this issue, in 2023 the Galvanized Autobody Partnership (GAP), a conglomerate of steel producers, automakers, resource companies, and galvanizing equipment manufactures convened by the International Zinc Association, initiated a research project with the University of Waterloo focused on characterizing the radiative properties of the coating throughout the galvannealing process. This ongoing research project elucidated the sensitivity of the radiative properties to specific aspects of the coating development, including coating solidification, increasing surface roughness, and the appearance of absorption features that appear to be connected to the appearance of specific intermetallic surface phases.

The outcome of this research project suggests that the sensitivity of the radiative properties of the coating to the evolving galvanneal coating may form the basis for online control. However, the complexity of the electromagnetic theory that connects the surface state to the radiative properties precludes the derivation of deterministic, physics-based instrument models. In this context, machine learning presents an opportunity to develop robust and computationally efficient instrument models that can translate measured radiative properties into real-time, industrially relevant coating attributes like roughness and iron concentration.

The objective of this AIST DSTM grant is to explore the possibility of integrating machine learning/artificial intelligence algorithms with online spectroscopic measurements into an approach for controlling the galvannealing process. This one-year project was structured around three complementary tasks. Task 1 focused on developing a spectral-emissivity library through controlled laboratory galvannealing experiments and accompanying metallurgical characterization. Spectral emissivity measurements were combined with coating-composition and surface-topography measurements to understand how the radiative properties, phase composition, and surface structure evolve during galvannealing.

Building on the resulting dataset, Task 2 focused on deriving physics-informed AI models capable of relating spectral emissivity features to coating composition. Feature-engineering techniques were used to identify wavelength regions sensitive to galvannealing progression, and machine-learning models were developed and evaluated using laboratory data.

Finally, Task 3 examined the industrial relevance of the developed approach through evaluation on independent industrial samples and assessment of future pathways toward deployment in continuous galvanizing lines.

2. Task 1: Spectral emissivity dataset for galvannealing progression

This task focused on establishing a dataset that connects spectral emissivity with galvannealing progression in zinc-coated interstitial-free (IF) steel. Zinc-coated IF samples obtained from our industry partner were processed in an Iwatani-Surtec galvanizing simulator at McMaster University. The galvannealing experiments were conducted at two processing temperatures (480°C and 540°C) and four annealing times (0, 15, 30, and 180 s), producing a range of coating conditions representative of different stages of galvannealing.

To fully characterize the resulting coating, *ex-situ* spectral emissivity measurements across the near-, mid-, and long-wave infrared regions were obtained using an Invenio-X FTIR spectrometer and combined with metallurgical characterization, including ICP measurements of coating Fe content, SEM/EDS analysis, and surface-topography measurements. A detailed description of the experimental and measurement procedure is provided in Appendix A. The combination of these measurements enabled direct comparison between radiative properties and the underlying topographical and morphological changes occurring during galvannealing.

2.1 Evolution of spectral emissivity during galvannealing

Figures 1 and 2 show the spectral emissivity of IF steel samples processed under different galvannealing conditions. The emissivity spectrum of the zinc-coated sample prior to galvannealing is also included as a baseline to assess the radiative-property changes associated with coating evolution.

Figure 1 compares the emissivity spectra obtained at 480°C and 540°C for annealing times ranging from 0 to 180 s. For the unannealed specimens, only minor differences in emissivity are observed, which reflect the as-received variability in the radiative properties. In both cases, the characteristic

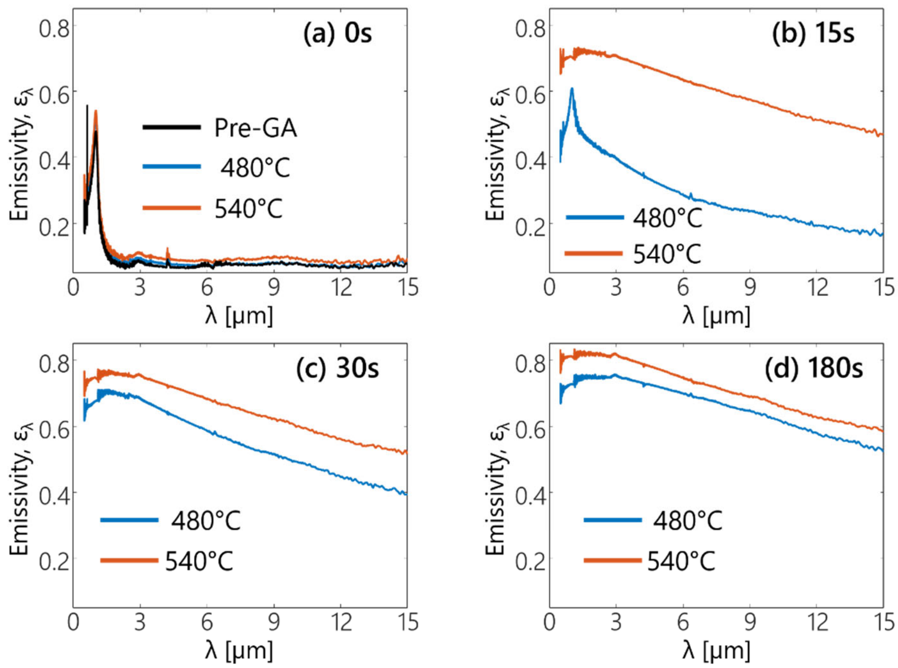

Figure 1. Spectral emissivity of the IF steel samples galvannealed at 480°C and 540°C for the following times: (a) 0 s, (b), 15 s, (c) 30 s and (d) 180s. The emissivity of the zinc-coated sample prior to galvannealing (Pre-GA) is included in (a) as a baseline for comparison.

zinc feature near 1 μm remains clearly visible. This feature is associated with an interband transition associated with the crystalline structure of solid zinc [1] and should therefore be viewed as an experimental artifact unlikely to be observed in spectra collected from continuous galvanized strip where the Zn coating is liquid. The emissivity changes radically as the galvannealing time increases, and the zinc feature becomes less pronounced and eventually disappears.

Figure 2 presents the same data grouped by processing temperature to illustrate the evolution of emissivity with annealing time. Similar trends are observed at both temperatures; however, the emissivity changes occur more rapidly for specimens annealed at 540°C. For example, the zinc feature near 1 μm is largely absent after only 15 s at 540°C, whereas it remains visible for the corresponding sample processed at 480°C. This suggests that increasing processing temperature accelerates the coating transformations responsible for the observed changes in radiative properties.

These results demonstrate that spectral emissivity evolves systematically with both processing temperature and annealing time. Changes in both emissivity magnitude and spectral shape are observed, indicating that the measured spectra contain information related to galvannealing progression. Therefore, to investigate the physical origins of the emissivity changes, the surface structure of the coatings is examined using scanning electron microscopy and laser-confocal topography measurements, while the coating composition is fully analyzed using inductively coupled plasma optical emission spectroscopy (ICP-OES).

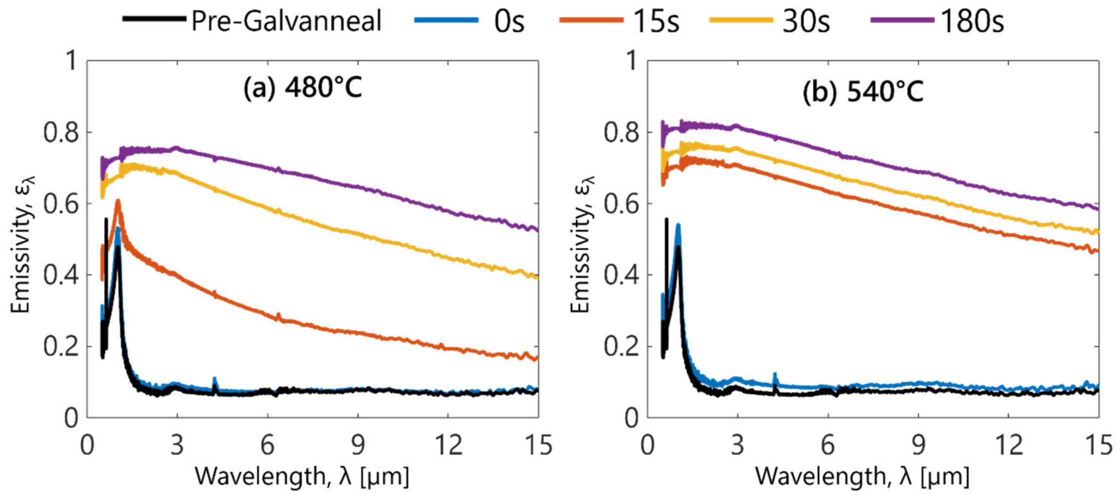

Figure 2. Spectral emissivity evolution with galvannealing time for (a) 480°C and (b) 540°C, illustrating the change in emissivity magnitude and spectral shape with increasing time.

2.2 Surface structure evolution

Figure 3 shows SEM images of all the galvannealing IF steel samples. The corresponding local Fe concentration measured using EDS is included for each sample to provide a qualitative indication of the accompanying compositional evolution.

The as-received specimens have coating surfaces that remain relatively smooth with the original zinc coating largely intact, which is consistent with the trend observed in the emissivity measurements, where the 1 μm zinc feature remains clearly visible. Rod-like intermetallic features, characteristic of early Zn–Fe intermetallic formation and commonly reported for zeta-dominant coatings [1], begin to appear across the surface after 15 s of galvannealing. For the 480°C sample, smooth regions remain visible between these features, suggesting incomplete transformation of the zinc coating, whereas the 540°C sample exhibits a more continuous transformed coating.

With increasing galvannealing time, the rod-like features gradually evolve into a more granular morphology, and the surface becomes increasingly interconnected. By 180 s, localized crater-like regions are observed, particularly for the 540°C samples, indicating heterogenous and non-uniform diffusive growth of the intermetallic layer with prolonged galvannealing [2]. The accompanying EDS measurements show a progressive increase in local Fe concentration with galvannealing severity, consistent with the observed morphological evolution.

Overall, the SEM results demonstrate that the coating evolves from a smooth zinc layer to a rough intermetallic surface. These observations provide qualitative evidence of coating evolution and motivate the quantitative surface-topography analysis presented in the following section.

2.3 Quantitative surface topography evolution

Figures 4 and 5 present optical micrographs obtained using a Keyence VK-X250 laser scanning confocal microscope and the corresponding surface height maps for the galvannealed IF steel samples. Consistent with the SEM observations, the optical micrographs also show that the surface topography evolves with longer heating time. The smooth zinc surface gradually gives way to

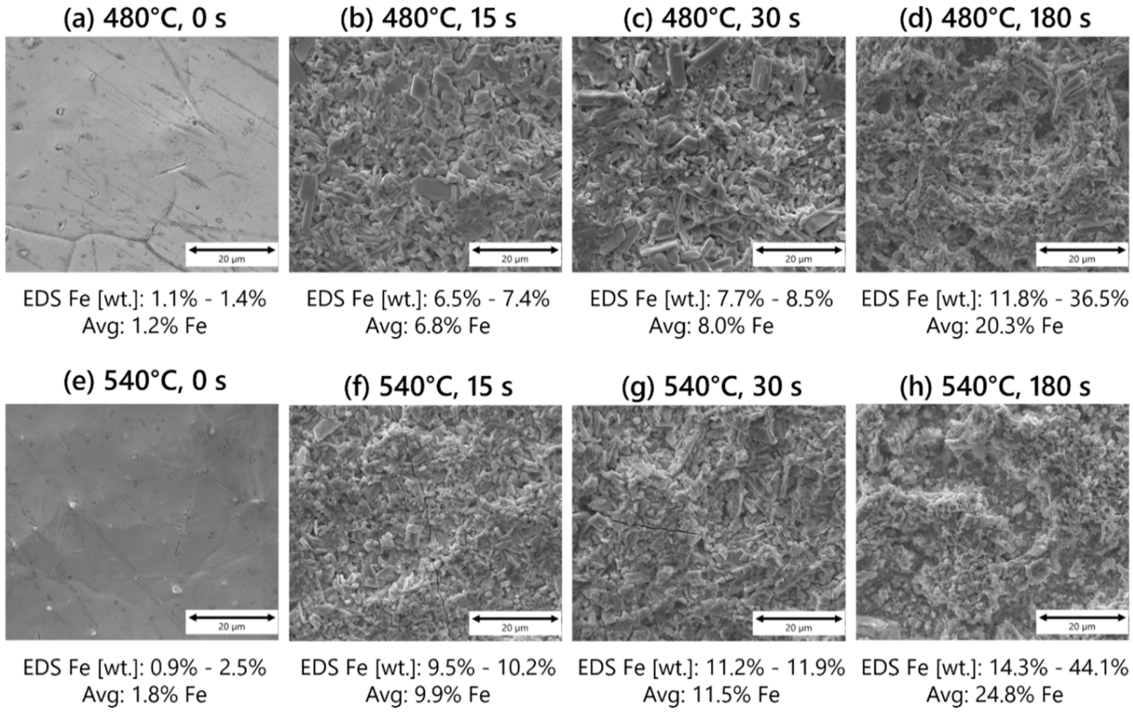

Figure 3. Scanning electron micrographs (SEM) of the IF samples galvannealed at 480°C (a, b, c, d) and 540°C (e, f, g, h). The corresponding average local Fe content measured by EDS is included for each sample.

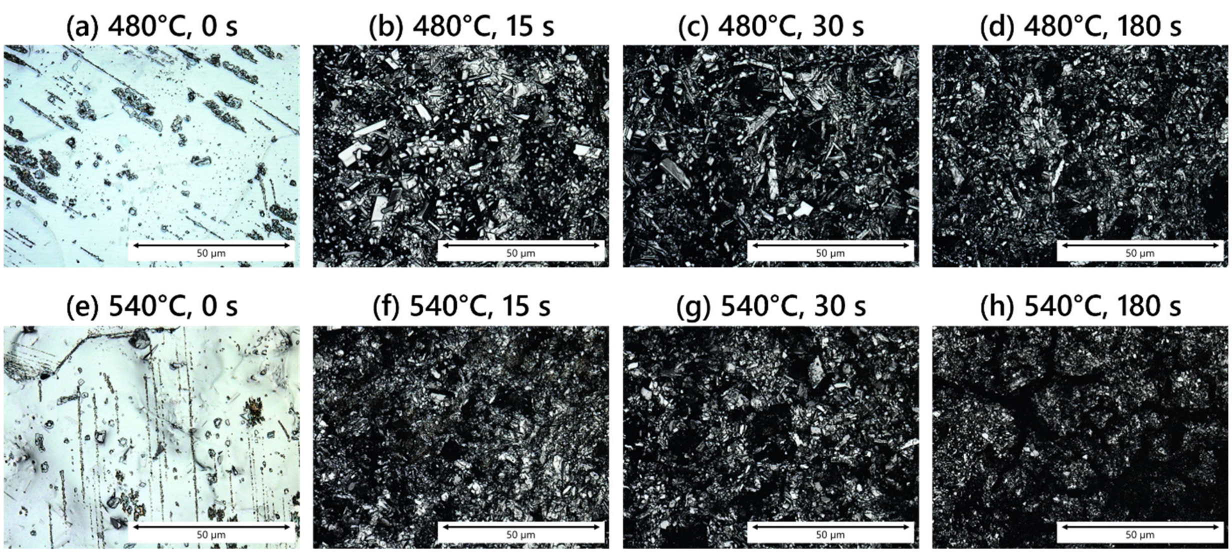

Figure 4. Optical-laser micrographs of the IF samples galvannealed at 480°C (a, b, c, d) and 540°C (e, f, g, h).

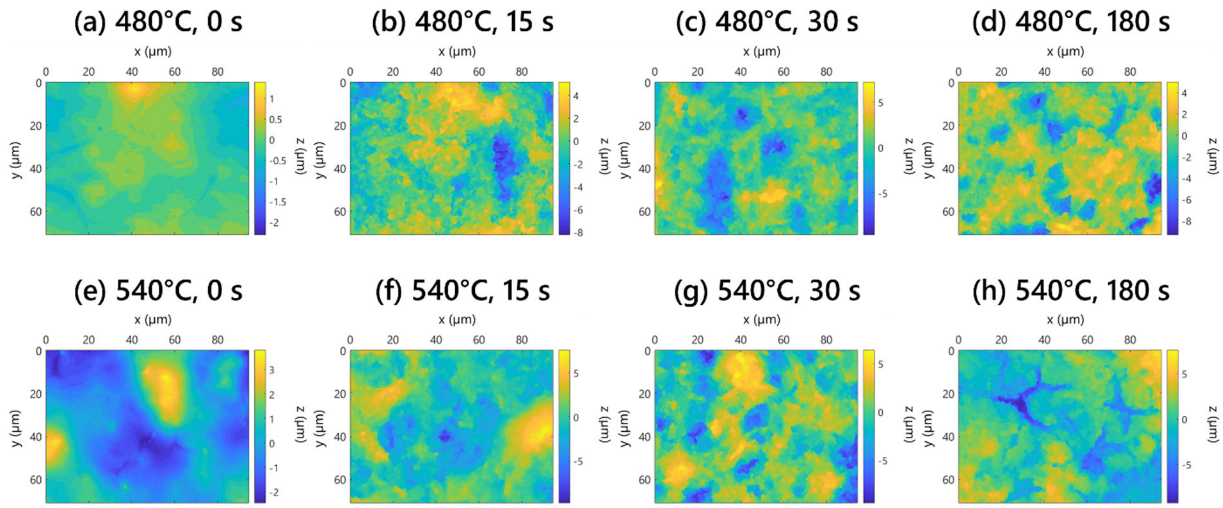

Figure 5. Corresponding surface height maps for the laser micrographs shown in Figure 4, illustrating the evolution of the topography with galvannealing time and processing temperature.

these morphological changes that are accompanied by measurable variations in surface height.

The RMS roughness and surface slope, calculated from the measured surface height maps using the equations in [3], are summarized in Figure 6. Error bars represent the variability across the nine measurement locations for each sample. Although both parameters capture changes in the surface topography, neither parameter changes monotonically with galvannealing time or processing temperature. In particular, the transition from rod-like to increasingly granular surface features observed in the SEM images is not captured by changes in either RMS roughness or surface slope alone.

The lack of a distinct trend suggests that conventional roughness descriptors capture only part of the topographical changes associated with the evolving coating surface. While the galvannealing

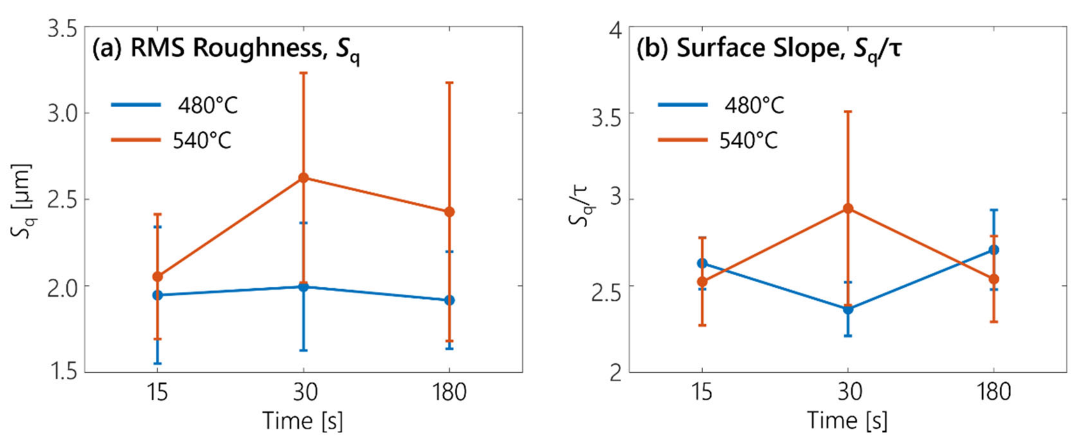

Figure 6. Summary of the quantitative surface-topography parameters obtained from the laser confocal measurements: (a) RMS roughness and (b) surface slope. Error bars represent one standard deviation of the mean value from nine locations on each sample.

process clearly modifies the surface topography, the transformation involves changes in both the feature morphology and the overall spatial distribution of features which may not be fully represented by these simple scalar roughness parameters. Therefore, scalar topographical descriptors alone might be insufficient for predicting the changes in the radiative properties during galvannealing.

2.4 Evolution of the coating composition

The galvannealed coating was chemically stripped from a 25 mm × 25 mm area of each sample, and resulting solution was analyzed by ICP to determine its Fe concentration. ICP was selected as the primary quantitative composition measurement because it provides a bulk, area-averaged determination of the coating Fe content following complete dissolution of the coating. This technique is also routinely used on continuous galvanizing lines to characterize galvanneal products for process monitoring and quality control. Although ICP does not directly distinguish the individual Zn–Fe intermetallic phases, the measured Fe content of the coating provides a practical measure of galvannealing progression because the formation of these phases is governed by the diffusion of Fe from the steel substrate into the Zn coating.

Figure 7 shows the measured Fe coating content as a function of processing condition. In contrast to the roughness parameters, the Fe content increases monotonically with annealing time. At a given annealing time, samples processed at 540°C consistently exhibited higher Fe content than the corresponding 480°C samples, indicating faster coating transformation at higher temperature. This trend is consistent with the temperature-dependent diffusion of Fe from the steel substrate into the zinc coating and the progressive formation of Fe-rich intermetallic phases.

The average Fe wt.% measured using EDS was also compared against the ICP results to evaluate whether EDS can track the progression of coating Fe enrichment during galvannealing. In contrast to ICP, EDS provides a rapid, non-destructive estimate of the Fe content that can be obtained

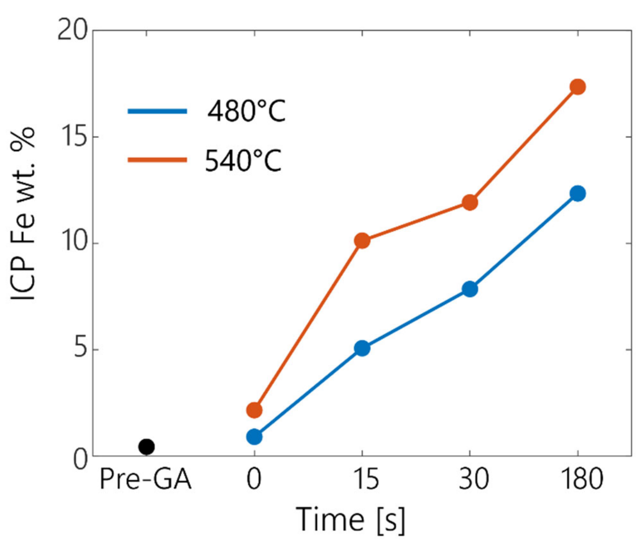

Figure 7. Bulk coating Fe content (in wt.%) measured by ICP for IF steel samples processed at 480°C and 540°C for annealing times ranging from 0 to 180 s. The zinc-coated pre-galvannealed (Pre-GA) sample was also analyzed as a baseline for comparison.

directly during SEM characterization. However, because the EDS interaction volume may extend beyond the coating into the steel substrate, it may overestimate the coating Fe content, especially for thin or cratered coatings. EDS is therefore evaluated in this study as a rapid semi-quantitative proxy for coating Fe enrichment rather than a replacement for the bulk composition measured by ICP.

Figure 8 compares the Fe wt.% measured by ICP and EDS. The dashed line represents the 1:1 relationship expected if both techniques produced identical Fe contents. The EDS-inferred concentration is generally consistent with the more accurate ICP values. The largest deviations are observed for the 180 s samples, where EDS reports substantially higher Fe contents than ICP. A linear fit to all samples produced a coefficient of determination (R^2) of 0.90, which increases to 0.97 when the 180 s samples are excluded. This suggests that EDS provides a good approximation of the relative Fe enrichment during the early and intermediate stages of galvannealing. The larger deviations at 180 s are likely associated with the evolved cratered coating morphology, which may cause the EDS interaction volume to extend beyond the coating and include a greater contribution from the steel substrate, resulting in an overestimation of the coating Fe content.

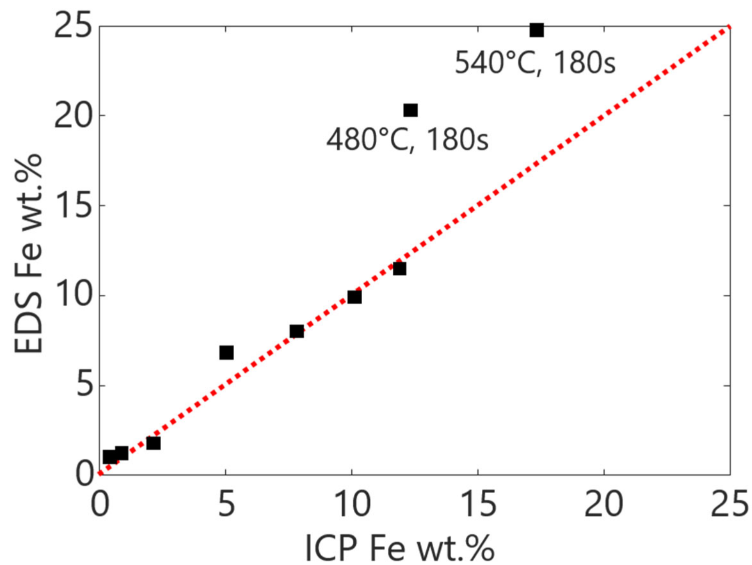

Figure 8. Comparison of coating Fe wt.% measured by ICP and EDS. The dashed identity line represents the 1:1 relationship between the two measurement techniques.

3. Task 2: Development of an emissivity-based coating composition model

Task 1 established that galvannealing produces systematic changes in spectral emissivity, surface structure, surface topography, and coating composition. The objective of Task 2 is to develop an instrument model capable of inferring parameters associated with the galvannealed coating directly from measured radiative properties of the coating. The evolution of Zn–Fe intermetallic phases during galvannealing influences the radiative properties through two interconnected mechanisms: (i) changes in the electronic properties of the coating, which modify its intrinsic optical properties, and (ii) topographical changes, which alter the absorption, reflection, and scattering of incident radiation.

The Fe content of the coating exhibited a clear monotonic relationship with processing conditions and is routinely used for industrial characterization and quality control of galvanneal products. Consequently, coating Fe content was selected as the primary target variable for model development. Task 2 therefore focused on extracting physically meaningful information contained within the measured emissivity spectra through feature engineering and physics-informed machine-learning models to accurately infer coating Fe content and, by extension, the progress in converting the Zn coating to the intermetallic layer.

3.1 Spectral feature engineering

The emissivity spectra shown in Figures 1 and 2 provide a physically meaningful description of the wavelength-dependent interaction between thermal radiation and the evolving galvanneal coating. However, the high spectral resolution provided by laboratory characterization techniques are not representative of the data that could be obtained from online measurements on continuous galvanizing lines, e.g. existing instrumentation used for measuring temperature. Consequently, spectral feature engineering was performed to develop a compact set of physically interpretable descriptors that preserve the information most relevant to galvannealing progression while reducing dimensionality, improving robustness to measurement noise, and remaining compatible with existing multispectral sensing systems.

To achieve this, the measured spectra were divided into five broad wavelength bands spanning the short-, mid-, and long-wave infrared regions (0–3 μm, 3–6 μm, 6–9 μm, 9–12 μm, and 12–15 μm). Partitioning the spectra into broad wavelength bands provides a practical representation of the measurements that could be realized on a continuous galvannealing line, potentially using commercially-available sensors, while allowing the correlation of the different spectral regions to galvannealing progression to be evaluated independently. It also provides a systematic framework for identifying the spectral regions most sensitive to coating Fe enrichment.

Numerous descriptors can be derived from each spectral band. However, for the purposes of this study, two key descriptors were investigated: (i) wavelength-weighted average emissivity and (ii) least-squares spectral slope. The wavelength-weighted average emissivity characterizes the overall change in the emissivity magnitude within each spectral band, while the least-squares spectral slope, obtained from a first-order linear regression of emissivity with wavelength, characterizes the local spectral shape within each wavelength band.

Figure 9 presents the wavelength-weighted average emissivity for each spectral band as a function of galvannealing time. The band-average descriptor exhibits a clear monotonic increase with increasing annealing time for both processing temperatures, consistent with the systematic increase in emissivity shown in Figures 1 and 2. Higher processing temperatures accelerate the evolution of the band-average emissivity, with largest increases occurring after only 15 s at 540 °C, reflecting the increased Fe diffusion and Zn–Fe intermetallic formation at the higher temperatures

Figure 10 shows the corresponding least-squares spectral slope for each wavelength band. Unlike the wavelength-weighted average emissivity, the spectral slope does not exhibit a simple monotonic relationship across all wavelength bands, reflecting the more subtle evolution of spectral shape during galvannealing. In particular, the first band (0 - 3 µm), which is distinct from

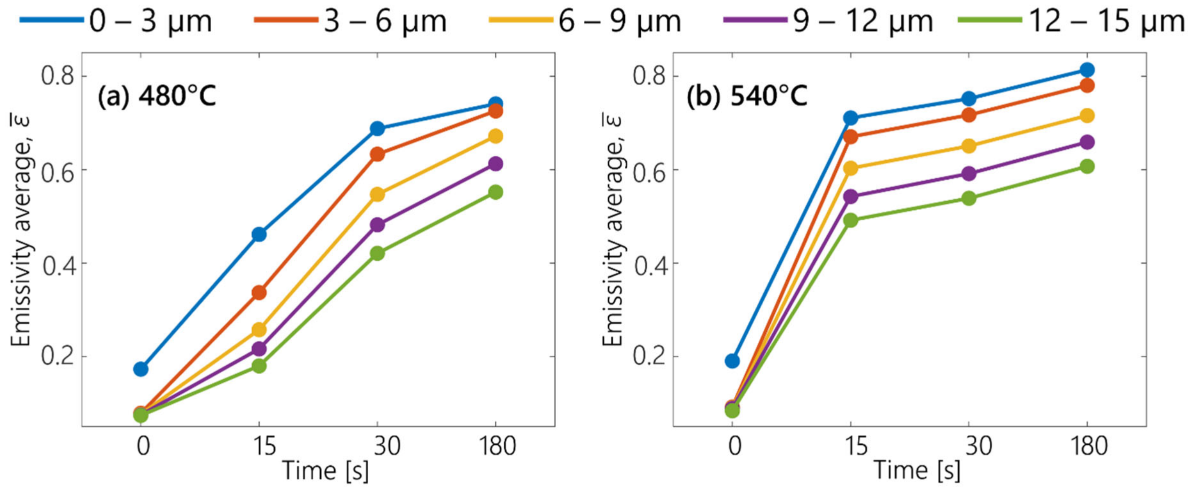

Figure 9. The wavelength-weighted average emissivity across the five spectral bands (0–3 µm, 3–6 µm, 6–9 µm, 9–12 µm, and 12–15 µm) for the IF samples galvannealed at **(a)** 480 °C and **(b)** 540 °C.

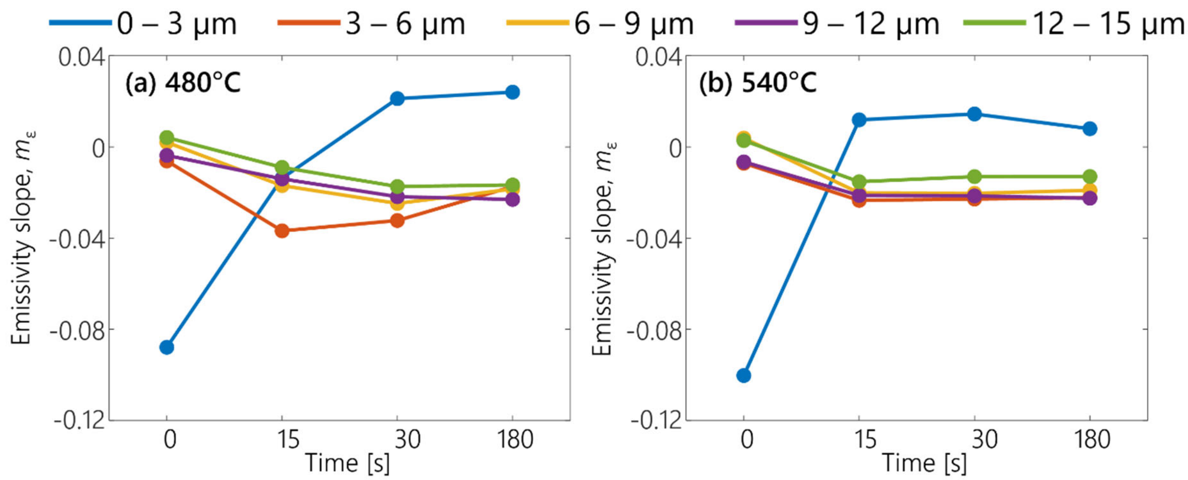

Figure 10. The least-squares spectral slope across the five spectral bands (0–3 µm, 3–6 µm, 6–9 µm, 9–12 µm, and 12–15 µm) for the IF samples galvannealed at **(a)** 480 °C and **(b)** 540 °C.

the remaining spectral bands, corresponds with progressive disappearance of the characteristic Zn feature at approximately 1 μm observed in Figures 1 and 2. This highlights that the spectral slope captures information related to galvannealing progression that is not represented by emissivity magnitude alone.

To evaluate the information contained within each engineered descriptor, correlation analysis was performed using the coating Fe content obtained from ICP. Table 1 summarizes the correlation coefficient, r, and residual standard deviation, σ_{res}, for each descriptor across the five wavelength bands. The quantitative analysis confirms the trends observed in Figures 9 and 10. For the wavelength-weighted average, progressively stronger correlations and lower residual scatter were obtained toward the longer wavelength regions, indicating that the LWIR bands retained the strongest relationship with coating Fe content. While the spectral slope exhibited more complex behaviour, its strongest relationship with coating Fe content was also obtained within the LWIR region, with the 9–12 μm band producing the lowest residual scatter.

Table 1. Pearson correlation coefficients (r) and linear regression residual standard deviations (σ_{res}) for the engineered spectral descriptors across the five wavelength bands relative to the measured ICP coating Fe content.

Band	**Wavelength-weighted average emissivity**		**least-squares spectral slope**	
	r	σ_{res}	r	σ_{res}
0 – 3 μm	0.944	0.092	0.840	0.028
3 – 6 μm	0.949	0.097	-0.493	0.010
6 – 9 μm	0.957	0.081	-0.789	0.007
9 – 12 μm	0.962	0.069	-0.910	0.003
12 – 15 μm	0.967	0.059	-0.823	0.005

Although band 5 (12–15 μm) produced the highest correlation for the wavelength-weighted average descriptor, band 4 (9–12 μm) was selected for subsequent model development because it provided the best overall balance between predictive performance, descriptor robustness, and practical implementation. In addition to exhibiting the lowest residual scatter for the spectral slope descriptor, this wavelength region aligns directly with the operating range of commercially available long-wavelength infrared sensors, making it well suited for future industrial deployment. Therefore, all subsequent development and evaluation of the inference models was focused on the 9–12 μm spectral band.

3.2 Physics-informed model development

Having identified the 9–12 μm spectral band as the most informative and practically relevant wavelength region, predictive models were developed to infer the Fe content in the coating from the engineered spectral descriptors. Several models were investigated to balance predictive performance, model interpretability, and suitability for future industrial implementation. The three representative models presented in this section were selected because they best illustrate the progression from a simple baseline model to a multivariate physics-informed machine-learning approach.

Since the experimental dataset consisted of only nine samples, careful evaluation of model performance was essential to fully exploit the information contained in the data while avoiding overfitting. This was accomplished using leave-one-out cross-validation (LOOVC), in which the model is trained repeatedly using eight of the nine samples while the remaining sample is used for testing, such that every sample is treated once as an unseen observation. This approach maximizes the amount of information available for model training while providing a robust estimate of predictive performance for small datasets.

The three representative models are summarized in Table 2. The linear model was first established as a baseline using the wavelength-weighted average emissivity. Although the relationship between the band average feature and galvannealing progression is monotonic, it is also nonlinear. Ultimately, a semi-logarithmic partial least squares (PLS) model was developed by combining both the wavelength-weighted average emissivity and the least-squares spectral slope. Unlike conventional linear regression, PLS projects correlated spectral descriptors onto a smaller set of latent variables that retain the information most relevant to coating Fe content, allowing the spectral slope to be incorporated while reducing feature collinearity.

Table 2. Leave-one-out cross-validation (LOOCV) performance of the representative models based on the coefficient of determination (R^2), root-mean-square error (RMSE), and maximum absolute prediction error.

Model	**Input features**	**R^2**	**RMSE (wt. %)**	**Max Error (wt. %)**
Linear	Average	0.87	1.96	4.62
Semi-log Linear	Average	0.92	1.53	3.17
Semi-log PLS	Average and Slope	0.90	1.76	2.66

Figure 11 compares the predicted and ICP-measured Fe content of the coating for each approach. The linear model successfully captures the overall trend but exhibits larger deviations at higher Fe contents, indicating that the spectral descriptors exhibit a monotonic but nonlinear relationship with coating Fe content. Consequently, applying a logarithmic transformation to the response variable improves the predictive accuracy, producing the lowest LOOCV RMSE. Incorporating the spectral slope through the semi-log PLS model further reduces the maximum prediction error, demonstrating that the spectral slope provides complementary information that improves the robustness of coating Fe prediction, particularly at higher Fe contents.

Overall, the evaluated models demonstrate that the engineered spectral descriptors contain sufficient information to accurately infer coating Fe content from emissivity measurements. Although the semi-logarithmic model achieved the lowest average prediction error, incorporating the spectral slope through the semi-logarithmic PLS model reduced the maximum prediction error while providing a flexible framework for incorporating additional physically meaningful spectral descriptors as more experimental and industrial data become available. For these reasons, only the semi-logarithmic linear and the semi-logarithmic PLS models are selected for subsequent evaluation in Task 3.

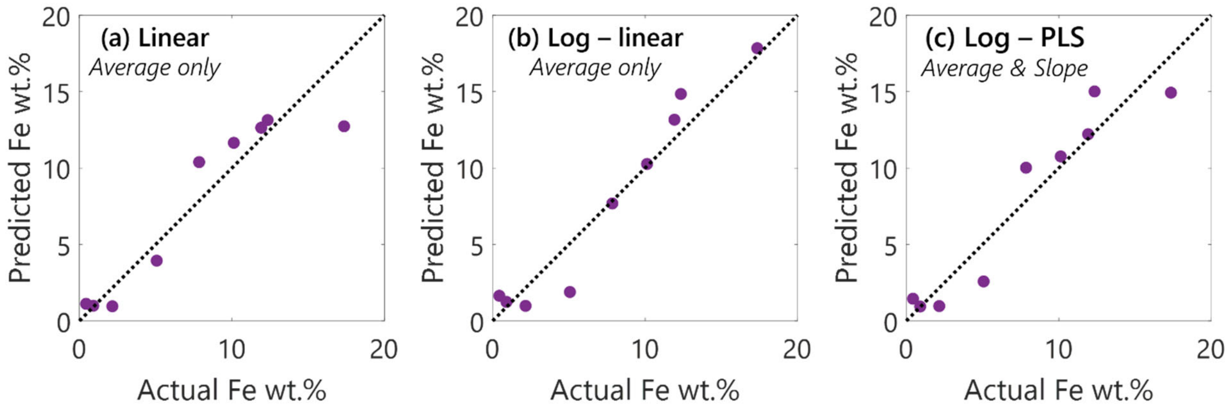

Figure 11. Parity plots comparing the predicted and measured coating Fe content obtained using (a) the linear model, (b) the semi-log model, and (c) the semi-log Partial Least Squares (PLS) model. The dashed line represents the one-to-one relationship between the predicted and measured coating Fe content.

4. Task 3: Assessment of generalizability and industrial applicability

Finally, the models derived in Task 2 are assessed by using them to analyze two specimens extracted from coils from an industrial continuous galvannealing process. Samples A and B represent low- and high-power galvannealing conditions, respectively, corresponding to coatings with and without retained zeta phase [1]. Both samples were independently characterized by the industrial partner using ICP as part of routine quality control. Sample A was also skin passed, which modifies the surface topography and thus the emissivity, thereby presenting a challenging assessment of model transferability. Table 3 summarizes the industrial samples used for validation.

Table 3. Summary of the independently processed industrial galvanneal samples used to evaluate the transferability of the developed emissivity-based inference model.

Sample	Processing condition	ICP Fe (wt. %)	Skin pass
A	Low GA furnace power (Zeta present)	8.7 – 10	Yes
B	High GA furnace power (No Zeta)	12.5 – 13.7	No

Figure 12 compares the measured spectral emissivity of the two industrial samples. Consistent with the findings presented in Tasks 1 and 2, the spectral emissivity is most sensitive to iron composition at the longer wavelengths, while the spectra are similar at shorter wavelengths. This observation further supports the selection of the 9–12 μm wavelength band (Band 4) for development of the Fe content inference model.

The inference models developed in Task 2 were subsequently applied emissivity spectra acquired from the industrial galvanneal samples using the FTIR system described in Task 1. The predicted Fe coating compositions were then compared with the ICP Fe ranges reported by the industrial partner, as shown in Figure 13. Although both models underestimated the absolute coating Fe content for the two industrial samples, only the semi-logarithmic PLS model preserved the correct ordering between the low- and high-power galvanneal coatings. For Sample A, both the semi-logarithmic linear and semi-logarithmic PLS models predicted Fe concentrations close to the

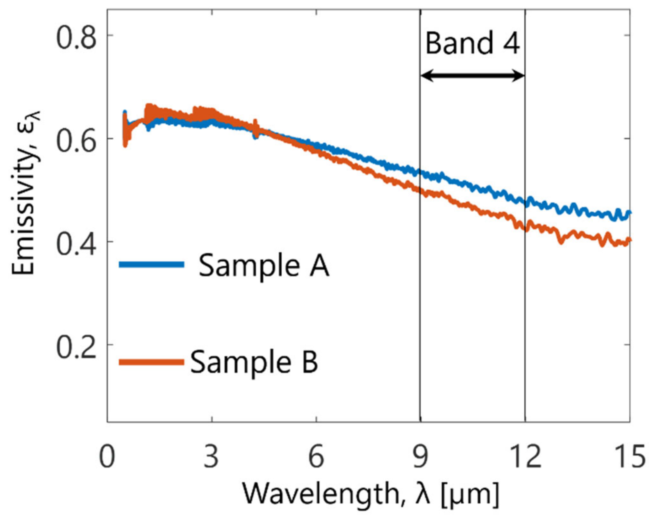

Figure 12. Spectral emissivity measurements for the two industrial galvanneal samples representing (A) low-power galvannealing with retained Zeta phase and (B) higher-power galvannealing with no Zeta phase. Each spectrum represents the average of four replicate measurements.

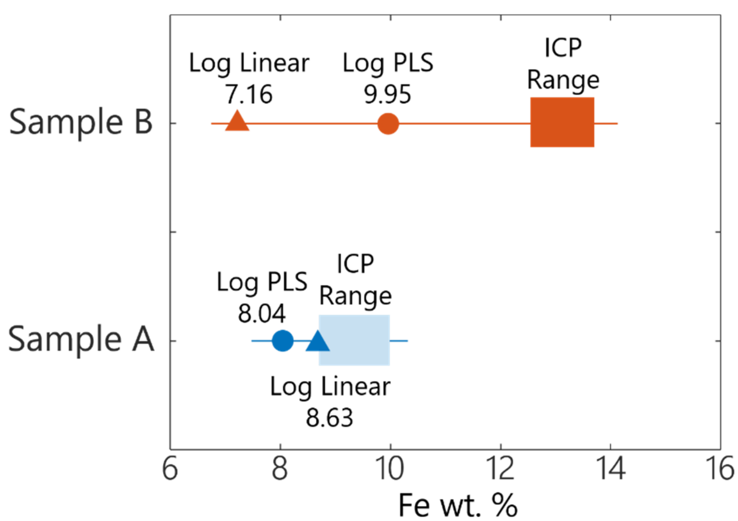

Figure 13. Comparison of the coating Fe contents predicted by the semi-log linear (Log Linear) and semi-log Partial Least Squares (Log PLS) models with the independently measured ICP Fe ranges for the two industrial galvanneal samples. The shaded boxes represent the ICP Fe ranges measured by the industrial partner, while the markers indicate the corresponding model predictions.

measured ICP Fe range, indicating that the wavelength-weighted average emissivity adequately described the spectral response for this lower-power galvanneal coating. In contrast, the models diverged for Sample B. The semi-logarithmic linear model substantially underpredicted the coating Fe content and predicted a lower Fe content than for Sample A, contradicting the ordering indicated by the ICP measurements. Incorporating the spectral slope through the semi-logarithmic PLS model increased the predicted Fe content for Sample B, restoring the correct ordering between the two galvanneal conditions.

Overall, these results demonstrate that spectral shape and emissivity magnitude capture different aspects of the radiative response of the evolving galvanneal coating, and that combining both descriptors enables the model to better distinguish between industrial coating conditions while providing a foundation for spectroscopic-based process monitoring on continuous galvanizing lines.

5. Future research directions

This research established the feasibility of online measurements of the galvanneal coating transformation from spectroscopic measurements. Several opportunities exist to further improve the developed inference framework and advance its application toward industrial process monitoring.

The first priority is to expand the database of paired spectral emissivity and coating Fe content measurements, spanning a broader range of coating Fe contents, galvannealing conditions, steel grades, coating weights, and surface processing conditions. A larger database would improve model robustness, enable calibration across a wider range of industrial operating conditions, and provide a more comprehensive assessment of model transferability. Future studies should also investigate *in-situ* high-temperature emissivity measurements during galvannealing to explicitly account for the coupled effects of temperature and phase evolution under representative production conditions.

The feature engineering results also indicate that the surface topography measurements contain richer information than is captured by the current descriptors. Although coating Fe content provided an effective initial target because of its monotonic relationship with galvannealing progression and its widespread industrial use, the evolving surface topography exhibits complex spatial morphology and heterogeneity that cannot be adequately described using conventional scalar roughness parameters alone. Future work should therefore investigate spatial descriptors derived directly from surface-height measurements, together with additional physically meaningful spectral descriptors, to better relate the evolving Zn–Fe intermetallic phases, surface morphology, and their corresponding radiative properties.

The developed inference framework provides an opportunity to complement existing process-monitoring strategies by directly estimating the coating state through online spectroscopic measurements. Unlike conventional characterization methods such as ICP, which require destructive offline analysis, the proposed approach relies entirely on non-contact radiative measurements, potentially using existing instrumentation, and therefore has the potential to provide continuous assessment of coating condition during production. Furthermore, whereas conventional process monitoring primarily infers galvannealing progression indirectly through process variables such as furnace temperature, the present work demonstrates the feasibility of estimating the evolving metallurgical state directly from the emitted thermal radiation. Because the methodology is based on physically meaningful spectral descriptors rather than a specific measurement instrument, it is readily transferable to alternative sensing platforms capable of measuring the required spectral information.

More broadly, by demonstrating that spectral emissivity contains sufficient information to infer galvannealing progression, the proposed framework establishes a new methodology for estimating the evolving metallurgical state of galvanneal coatings directly from spectroscopy, providing a foundation for future non-contact monitoring and process control of galvanneal products

6. Dissemination of results

The outcomes of this project have been disseminated to both academic and industrial audiences. The developed inference framework and its preliminary industrial validation were presented at the AISTech 2026 Conference. This present report provides a comprehensive summary of the project outcomes and establishes a foundation for future peer-reviewed publications on emissivity-based monitoring of galvanneal coatings. Continued dissemination through AIST conferences and journal papers will further promote the adoption of digital sensing and machine-learning methodologies for advanced steel manufacturing.

7. Student participations

Student participation was central to every stage of the project. Graduate and undergraduate researchers planned and executed the experimental campaigns, collected spectral emissivity measurements, performed surface topography characterization, coordinated coating chemistry analysis, developed the inference models, and validated the methodology using independently processed industrial samples. Through these activities two postdoctoral researchers and two graduate students acquired interdisciplinary expertise spanning heat transfer, spectroscopy, machine learning, data analytics, surface metrology, and steel processing.

Beyond the technical work, these personnel gained practical experience in project management, teamwork and scientific communication. The project also provided opportunities for these personnel to present their work at AISTech 2026 and engage directly with steel industry professionals, strengthening both their professional networks and understanding of digital transformation within modern steel manufacturing.

By leading the entire project from experimental design through to industrial validation, these personnel developed not only advanced technical expertise but also a practical understanding of how research can be translated into solutions for the steel industry.

8. Steel plant interaction

Close collaboration with the industrial partner ensured that the research outcomes remained relevant and aligned with practical industrial challenges throughout the project. Site visits to Stelco Hamilton Works provided the personnel with first-hand exposure to galvannealing operations, coating quality assessment, and the practical constraints associated with online process monitoring. Discussions with plant personnel provided valuable insight into current production practices and future monitoring requirements, while also helping to guide the selection of practically relevant spectral features, validation strategies, and future directions for industrial implementation. The industrial partner also supplied all the IF steel samples used throughout the project, supporting the development of the phase-resolved spectral-emissivity library (Task 1), the emissivity-based inference framework (Task 2), and the independent industrial validation (Task 3).

9. Project timeline

The major project activities completed during the reporting period are summarized in Table 4.

Table 4. Timeline of the major project activities completed during the development and validation of the inference framework between September 2025 and June 2026.

	Sep	**Oct**	**Nov**	**Dec**	**Jan**	**Feb**	**Mar**	**Apr**	**May**	**Jun**
Task 1										
Sample preparation & galvannealing										
Spectral emissivity measurements										
Surface & coating characterization										
Phase-resolved database development										
Task 2										
Spectral feature engineering										
Model development										
Cross-validation & model selection										
Task 3										
Industrial sample characterization										
Industrial model validation										
Final reporting & dissemination										

10. Project cost

The AIST Foundation funding leveraged existing laboratory infrastructure, university facilities, and industrial partnerships to complete the experimental, analytical, and dissemination activities described in this report. Existing research equipment and facilities were utilized wherever possible, allowing the project funding to be directed primarily toward personnel salaries, experimental characterization, travel, and project-related consumables. The approximate allocation of the project budget is as follows:

Salaries (USD $18,000; 60%): Most of the budget supported graduate student researchers conducting experimental campaigns, spectral characterization, data analysis, machine-learning model development, industrial validation, and preparation of technical publications and reports.

Equipment and characterization (USD $7,500; 25%): galvannealing experiments, SEM/EDS characterization, FTIR measurements, ICP coating chemistry analysis, laboratory consumables, specimen preparation, and other experimental costs associated with developing the spectral-emissivity database.

Travel and knowledge dissemination (USD $3,000; 10%): Supported student travel for collaboration with industrial partners, site visits to continuous galvanizing facilities, and presentation of project outcomes at AISTech 2026.

Miscellaneous consumables (USD $1,500; 5%): This includes miscellaneous expenses, consumables and specimen preparation supplies.

11. Student employment in the steel industry

Although no student participants have yet accepted full-time employment within the steel industry, the project has significantly strengthened the pipeline of highly qualified personnel pursuing steel-related careers. One master's student who participated in the project successfully completed their MASc degree and subsequently accepted an offer to continue into a PhD focused on galvannealing and continuous galvanizing line research. The remaining graduate students also continue to conduct research related to advanced steel manufacturing, further developing the experimental, analytical, and industrial expertise relevant to future careers in the steel industry.

12. Future of grant

The plans contained in the original proposal are now complete. I have ~$10,000[1] remaining and request permission to continue promoting the steel industry to engineering students at my university using these funds. I agree to provide an annual report to AIST until the funds are depleted.

The plans contained in the original proposal are now complete. I agree to the final results being posted to the AIST website, shared with other universities, shared with AIST members, added to the AIST Library, or presented at a conference.

____

Signature of Professor and Date

[1] These funds are committed to the salaries of project personnel and will be exhausted by August 31, 2026.

13. References

[1] M. Kagaya, F. K. Suleiman, A. P. Domingos Cardoso, J. R. McDermid, and K. J. Daun, "Connecting surface microstructure to the radiative properties of galvannealed steel," Materials Characterization, 116449, 2026.

[2] P. M. Hale, R. N. Wright, and F.E. Goodwin, "The Role Of "Cratering" in the processing and properties of galvannealed steel sheet," SAE Trans., vol. 110, p. 72–76, 2001.

[3] N.S. Narayanan, An Investigation into Radiative Property Variations Across Pre-annealed Advanced High Strength Steel Coils, University of Waterloo, 2023. MASc Thesis.

[4] J.R. Howell, M.P. Mengüç, K.J. Daun, and R. Siegel, Thermal Radiation Heat Transfer, CRC Press, Boca Raton, FL, 2021.

Appendix A: Experimental and measurement procedure

Industrially prepared Zn-coated interstitial-free (IF) steel samples were cut into 120 mm × 200 mm panels and galvannealed in the Iwatani-Surtec galvanizing simulator. All samples were heated at a target ramp rate of 20 °C/s to the peak galvannealing temperatures of either 480 °C or 540 °C and then held for annealing times of 0, 15, 30, or 180 s. After galvannealing, the edges of the panels, which may experience non-uniform heating, were removed before the central region was sectioned for subsequent characterization.

Following the heat treatment, all surface topography, radiometric, and coating composition measurements were performed on the surface corresponding to the top of the steel coil. Prior to characterization, all samples were cleaned using ethanol and acetone. SEM images and EDS maps were acquired using a FEI Quanta FEG 250 equipped with an Oxford Instruments x-act detector. EDS maps were acquired from three representative locations on each sample. Surface profile measurements were performed using a Keyence VK-X250 laser scanning confocal microscope, which generated three-dimensional surface height maps over a 95 µm × 71 µm area. Tilt correction was performed using the Keyence FileAnalyzer software. Nine inspection locations were analyzed for each sample to determine the average scalar roughness parameters.

Coating Fe content was determined using inductively coupled plasma optical emission spectroscopy (ICP-OES). Prior to chemical stripping, the reverse side and edges of each specimen were masked to ensure that only the galvanneal coating on the measurement surface was dissolved. The coating was selectively stripped using a 10 vol.% H_2SO_4 solution containing 2.5 g/L hexamethylenetetramine (HMTA), which minimizes dissolution of the steel substrate. The resulting solutions were analyzed using ICP-OES. Matrix-matched calibration standards spanning the expected Fe concentration range were prepared and analyzed alongside the samples to improve analytical accuracy.

Spectral radiative properties were measured using a Bruker Invenio-X FTIR spectrometer with a Spectralon-coated integrating sphere (0.5–1.1 µm) and an Infragold-coated integrating sphere (1.1–15 µm) to obtain the near-normal directional-hemispherical spectral reflectance (ρ_λ). The near-normal spectral emissivity, ε_λ, is then calculated using Kirchhoff's law, $\varepsilon_\lambda = 1 - \rho_\lambda$ [4]. The FTIR spectrometer has ±2% calibration uncertainty and less than ±1% repeatability. Two measurements were acquired from different locations on each laboratory sample and averaged, whereas the reported emissivity spectra for the industrial galvannealed samples used for model validation represent the average spectra measured from four separate samples collected from the same coil.

14. Appendix B: Letter of support from industry partner

STELCO
The Steel Company of Canada
386 Wilcox Street
PO Box 2030
Hamilton, ON L8N 3T1
905.528.2511
stelco.com

Letter of Support

Acceptance of University of Waterloo's Work:

"AI-Driven Radiative Sensing for Optimizing Continuous Galvanizing Processes"

To Whom It May Concern,

On behalf of Stelco, I am pleased to accept and express our support for the work completed by the University of Waterloo entitled "AI-Driven Radiative Sensing for Optimizing Continuous Galvanizing Processes." This project, funded by AIST's *Digital Technologies for Steel Manufacturing Grant*, represents an advancement in applying artificial intelligence and radiative sensing technologies to optimize continuous galvanizing operations within the steel manufacturing industry.

Sincerely,

Chris Martin-Root

Director of Strategic Planning and Research